

# Melting Behavior of Ethylene–Tetrafluoroethylene Alternating Copolymer

RACHELE PUCCIARIELLO

Dipartimento di Chimica, Università della Basilicata, Via N. Sauro 85, 85100 Potenza, Italy

## SYNOPSIS

The melting behavior of the alternating copolymer of ethylene and tetrafluoroethylene (ETFE) was investigated by differential scanning calorimetry (DSC). A complex melting pattern is observed, strongly influenced by the thermal history. Three melting processes can be identified, whose heats of fusion and peak temperatures ( $T_{m1'}$ ,  $T_{m1}$ , and  $T_{m2}$  at increasing values) strongly depend upon thermal treatments. The higher-temperature melting peak  $T_{m2}$  is not affected by the crystallization conditions (i.e., cooling rate and annealing); therefore, it can be attributed to more perfect crystals present in the original sample. The peak at  $T_{m1}$  increases when the cooling rate is decreased and upon prolonged and/or higher-temperature annealing, and it fastly merges to the higher-temperature peak at  $T_{m2}$ . The peak at  $T_{m1}$  can be due to crystals that are able to recrystallize and perfect during thermal treatments. Lastly, the peak at the lowest-temperature  $T_{m1'}$ , produced only by annealing and strongly developing on increasing annealing time and temperature, is the so-called annealing peak that can be attributed to much poorer crystallites grown among the larger ones. The melting behavior of ETFE is compared with that of the ethylene–chlorotrifluoroethylene (ECTFE) alternating copolymer. © 1996 John Wiley & Sons, Inc.

## INTRODUCTION

Ethylene–tetrafluoroethylene (ETFE) and ethylene–chlorotrifluoroethylene (ECTFE) alternating copolymers are thermoplastic materials having good electrical and mechanical properties, high chemical resistance, good processability, and outstanding thermal stability. Extensive structural and dynamic mechanical studies have been performed on ETFE copolymers<sup>1–7</sup>; nevertheless, few articles have been published about the melting behavior,<sup>5,6,8</sup> although its knowledge is particularly important as it plays a key role in the processing and use conditions of materials. In particular, the dependence of the melting temperature upon the copolymer composition has been reported. A maximum has been pointed out for the 50/50 copolymer and a minimum for tetrafluoroethylene content in the range 60–70 mol %.<sup>5,6</sup> The peculiar dependence of melting points on composition, i.e., the decrease of the melting point as tetra-

fluoroethylene content increases above 50 mol %, allows the practical utilization of the more fluorinated copolymers, which possess higher chemical and aging resistance.<sup>5</sup>

The structure and the dynamic mechanical properties of ECTFE copolymers have been deeply investigated.<sup>9–12</sup> Also, a detailed analysis of the melting of 50/50 ECTFE has been performed during a study of the effect of high-temperature aging on the physicochemical characteristics of the copolymer.<sup>13</sup> Differential scanning calorimetry (DSC) revealed single or double melting peaks, depending upon the thermal history. The lower-temperature melting peak was produced only by thermal treatments and was strongly dependent on annealing time and temperature, while the high-temperature one was independent of the crystallization conditions (i.e., quenching, slow cooling, or even annealing).

In this article, we report a study by DSC of the thermal behavior of an ETFE alternating copolymer by investigating the effect of the thermal history on the melting pattern and compare this behavior to the melting of an ECTFE alternating copolymer.

## EXPERIMENTAL

### Materials

The materials used for this work are

- (A) A powder sample of a 43/57 ethylene/tetrafluoroethylene (ETFE) alternating copolymer (Halon ET 102, Ausimont) with a nearly complete alternation (higher than 90%) between the two comonomers;
- (B) A 50/50 ethylene/chlorotrifluoroethylene (ECTFE) (in the form of pellets) alternating copolymer (Halar 500, Ausimont), consisting of 85 mol % alternating (crystallizable) units and the remaining consisting of non-crystallizable short blocks of ethylene and chlorotrifluoroethylene.

### Thermal Analysis

Thermal analysis was performed by a differential scanning calorimeter (DSC 7, Perkin-Elmer) equipped with a 1020 personal integrator. All runs were performed on  $10 \pm 0.5$  mg samples in a nitrogen atmosphere. Melting temperatures were given as the maxima of the peaks. They were checked using the melting temperatures of indium ( $156.6^\circ\text{C}$ ), tin ( $231.8^\circ\text{C}$ ), lead ( $327.4^\circ\text{C}$ ), and zinc ( $419.5^\circ\text{C}$ ) and are reproducible to  $\pm 0.5^\circ\text{C}$ . Heats of fusion were calculated from peak areas using a standard software, calibrated with benzoic acid ( $\Delta H_m = 141.7$  J/g) and their uncertainty is  $\pm 1$  J/g. The base line was optimized in the range from 150 to  $300^\circ\text{C}$  and subtracted from the curves.

Before the measurements, the samples were taken to  $300^\circ\text{C}$  at  $10^\circ\text{C}/\text{min}$  and cooled to room temperature at the same scanning rate. The annealing was performed in the DSC apparatus in a nitrogen atmosphere for times ranging from 1 to 5 h at 150, 180, and  $200^\circ\text{C}$ .

## RESULTS AND DISCUSSION

In Figure 1(A)\* the DSC scan from 200 to  $300^\circ\text{C}$  performed at  $10^\circ\text{C}/\text{min}$  for as-polymerized ETFE is reported. The copolymer shows a single melting endotherm ( $T_m = 255.4^\circ\text{C}$ ,  $\Delta H_m = 29.06$  J/g). The

\* In the figures reporting the DSC scans, just the peaks are shown, although the heats of fusion have been calculated taking into account the whole pre-fusion interval (i.e., starting from  $150^\circ\text{C}$ ).

DSC curve obtained on reheating at  $10^\circ\text{C}/\text{min}$  the melt-crystallized material (i.e., the material kept to  $300^\circ\text{C}$  at  $10^\circ\text{C}/\text{min}$  and cooled to room temperature at the same scanning rate) reveals a doublet melting pattern, the lower-temperature melting peak at  $T_{m1} = 246.4^\circ\text{C}$  and the higher-temperature one at  $T_{m2} = 257.4^\circ\text{C}$  (Figure 1(B)). The total heat of fusion  $\Delta H_m = 18.47$  J/g, less than the value obtained for the never-melted copolymer, as in PTFE<sup>14-21</sup> and other TFE copolymers,<sup>22-24</sup> denotes that the melt-crystallization causes a decrease in the polymer crystallinity (i.e., lower crystallinity is achieved from melt-crystallization as compared to the in-reactor polymerization crystallization). This behavior, in the case of PTFE, has been attributed to the poor molecular mobility of the melt resulting from the very high melt viscosity.

To study how the melting peaks are affected by the thermal history, we applied different crystallization conditions, i.e., "quenching" (cooling from the melt at the maximum rate allowed by the instrument) or used various cooling rates (50, 20, 10, 5, and  $3^\circ\text{C}/\text{min}$ ). In Figure 2, the DSC curves obtained on reheating at  $10^\circ\text{C}/\text{min}$  the samples crystallized at the different cooling rates are reported. The doublet melting pattern is always present, although the two peaks show different relative extents depending on the thermal history. In particular, the low-temperature peak becomes less and less evident on passing from the fast crystallization ("quenching") [Fig. 2(e)] to the slow one ( $3^\circ\text{C}/\text{min}$ ) [Fig. 2(a)]. In Figure 3 the peak temperatures  $T_{m1}$  and  $T_{m2}$  and the total heat of fusion  $\Delta H_m$  are shown as a function of the cooling rate,  $V_{\text{cool}}$ .  $\Delta H_m$  and  $T_{m2}$  are nearly constant, while  $T_{m1}$  slightly increases on decreasing the cooling rate. The trends of  $T_{m1}$  and  $T_{m2}$  as a function of  $v_{\text{cool}}$  clearly indicate that the good crystals (those melting at  $T_{m2}$ ) anneal less than do the poorer ones (those melting at  $T_{m1}$ ).

To understand the chance of reorganization of crystals during heating, scans at variable heating rates (5, 10, 20, 50, and  $80^\circ\text{C}/\text{min}$ ) were carried out on the melt-crystallized copolymer. The double melting pattern is recognizable up to  $20^\circ\text{C}/\text{min}$ . For higher heating rates, the two peaks coalesce into only one (most likely due to thermal lags within the sample and thus loss in resolution). The peak temperatures ( $T_{m1}$  and  $T_{m2}$ ) are reported as a function of the heating rate,  $V_{\text{heat}}$ , in Figure 4.  $T_{m1}$ , when observable, and  $T_{m2}$  increase upon increasing the heating rate. This behavior is evidence for superheating, which can take place when the crystal melting rate is lower than the heating rate.

To better investigate the nature of the melting

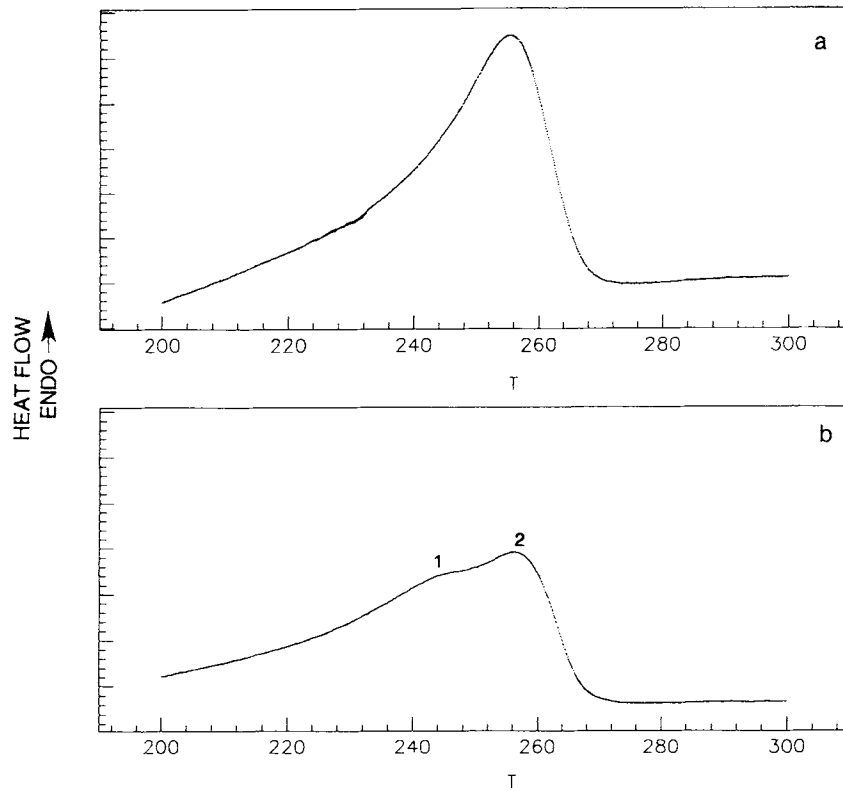


**Figure 1** DSC curves from 200 to 300°C for ETFE: (a) native sample; (b) melt-crystallized sample. Temperature is expressed in °C. The heating rate is 10°C/min. Peaks 1 and 2 are indicated.

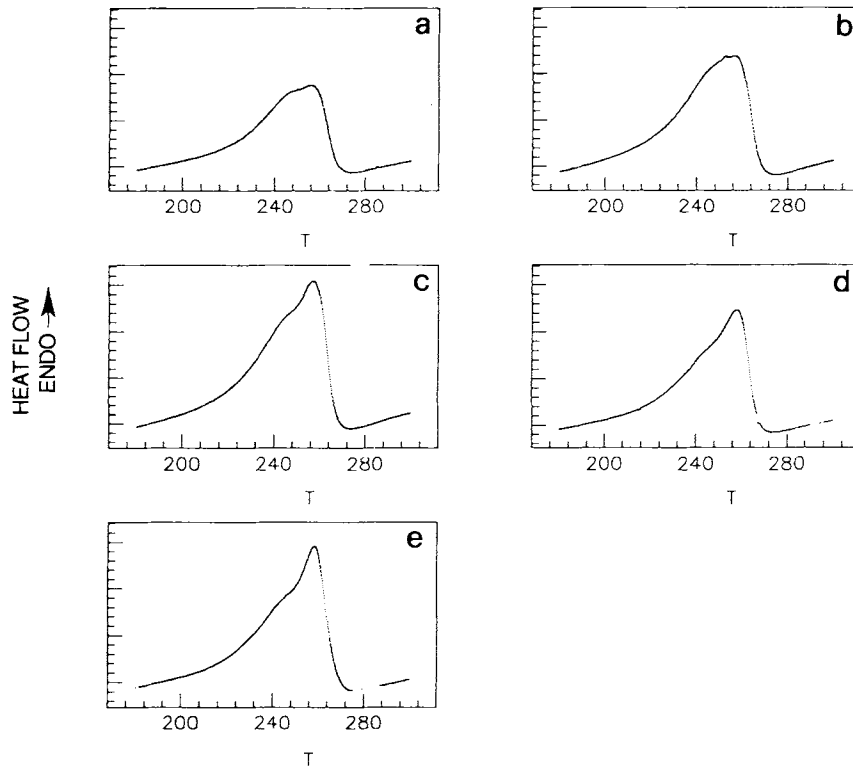


**Figure 2** DSC curves obtained on reheating at 10°C/min the samples of ETFE crystallized from the melt at the following cooling rates: (a) 3, (b) 5, (c) 20, and (d) 50°C/min and (e) “quenched.” Temperature is expressed in °C.

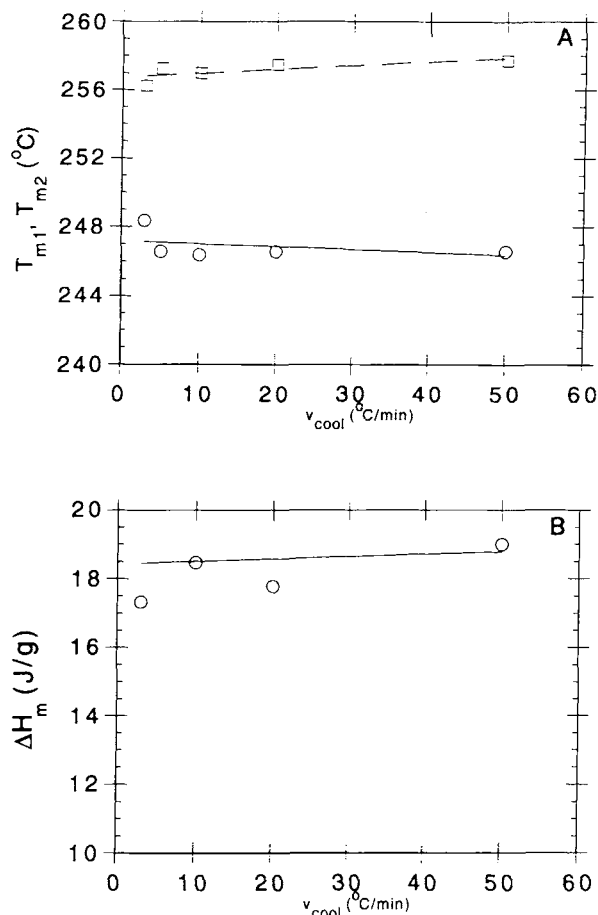


**Figure 3** (A) Peak temperatures (°C) (○)  $T_{m1}$ ; (□)  $T_{m2}$  and (B) heat of fusion  $\Delta H_m$  (J/g) as a function of the cooling rate (°C/min) for ETFE.

peaks, the samples were submitted to isothermal annealing at  $T_a = 150, 180,$  and  $200^\circ\text{C}$ , for times ( $t_a$ ) in the range from 1 to 5 h. In Figure 5, the DSC curves recorded on reheating at  $10^\circ\text{C}/\text{min}$  the annealed samples are reported. At  $T_a = 150$  and  $180^\circ\text{C}$ , the previously described doublet melting pattern is still observable. Nevertheless, for the longer annealing times, the higher-temperature peak at about  $258^\circ\text{C}$  is very clear, while the lower-temperature one at about  $246^\circ\text{C}$  is just recognizable. On increasing the annealing temperature and/or the annealing time, the double melting pattern disappears; in particular, only the higher-temperature peak is observable. The lower-temperature one is likely to be shifted to higher temperature, merging to the higher one. At  $T_a = 180^\circ\text{C}$ , another endotherm at  $T_{m1}' = 198^\circ\text{C}$  appears. This peak, in contrast to the main one which is not influenced by annealing, strongly

develops on annealing; in fact, prolonged annealing and/or higher-temperature annealing cause this peak to become more intense and shifted to higher temperatures. This peak is present in many macromolecules and occurs several degrees above the annealing temperature; therefore, it is often called the "annealing peak."<sup>25</sup> In Figure 6, the peak temperatures  $T_{m1}'$  and  $T_{m2}$  are shown as a function of the annealing time at the different annealing temperatures. As previously observed,  $T_{m2}$  is not changed by the thermal treatments, while  $T_{m1}'$  increases on annealing. Moreover, also, the total heat of fusion  $\Delta H_m$  increases on annealing time and temperature, as seen in Table I, where the most important data obtained in our analysis are summarized.

The previously described experimental results reveal a complex melting behavior for the ETFE copolymer. Multiple melting peaks have been observed for many crystallizable polymers and have been attributed to a number of causes such as the presence of the distribution of two or more crystalline dimensions, different molecular weight species, reorganization during the heating, presence of crystals with different stability, and polymorphism.<sup>25</sup> In our case, the following features can be observed:

1. A main peak (2) which is not affected by the crystallization conditions (i.e., cooling rate and annealing temperature and time).
2. A lower-temperature peak (1) that increases its temperature merging to the higher-temperature one for lower cooling rates and, probably, for higher annealing temperatures or/and times.

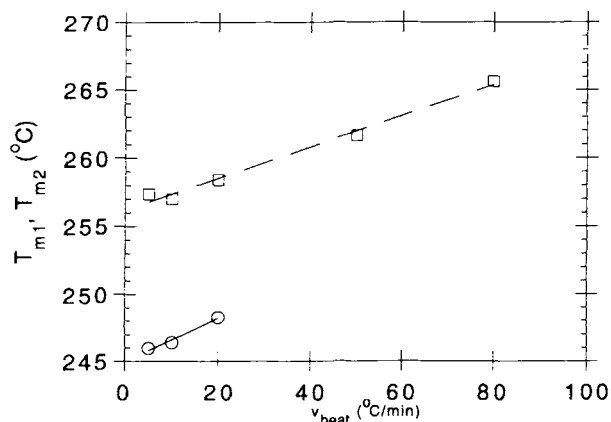


**Figure 4** Peak temperatures (°C) (○)  $T_{m1}$ ; (□)  $T_{m2}$  as a function of the heating rate (°C/min) for ETFE.

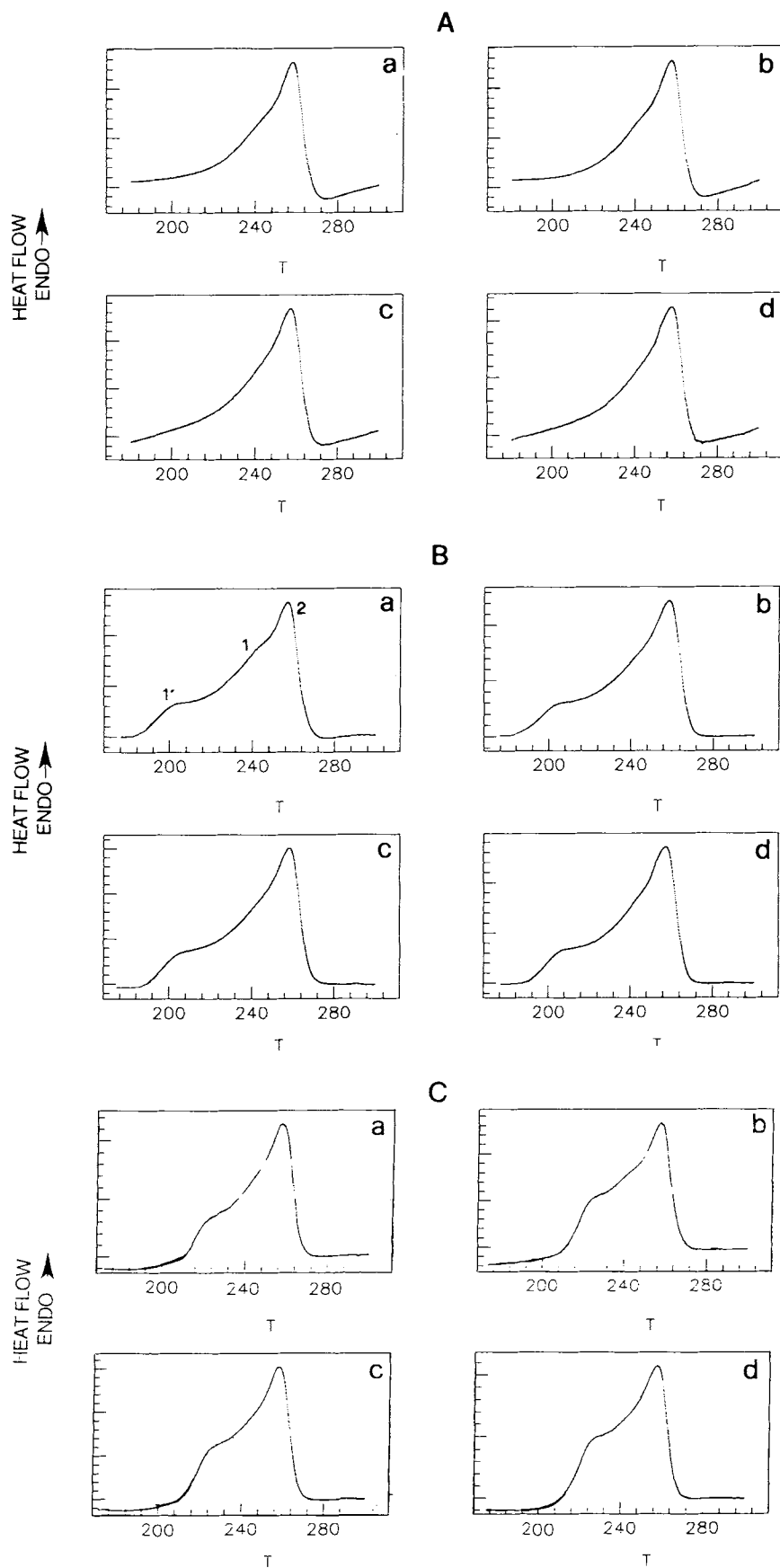


**Figure 5** DSC curves obtained on reheating at 10°C/min the samples of ETFE annealed at (A) 150, (B) 180, and (C) 200°C for the following annealing times: (a) 1, (b) 2, (c) 3, and (d) 5 h. Temperature is expressed in °C. Peaks 1', 1, and 2 are shown.

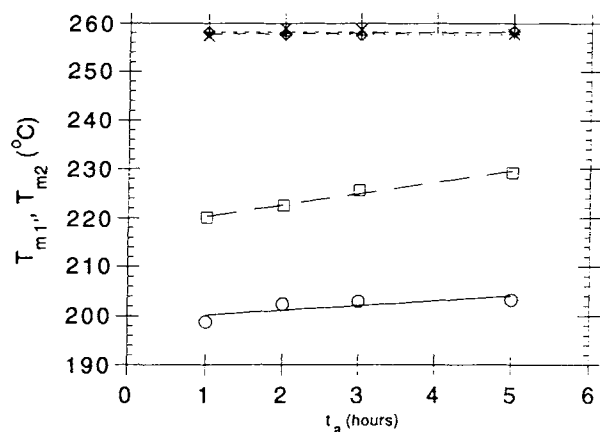


**Figure 6** Peak temperatures ( $^{\circ}\text{C}$ ) as a function of the annealing time (h) for ETFE.  $T_{m1'}$ : ( $\circ$ )  $T_a = 180^{\circ}\text{C}$ , ( $\square$ )  $T_a = 200^{\circ}\text{C}$ ;  $T_{m2}$ : ( $\times$ )  $T_a = 150^{\circ}\text{C}$ , ( $\diamond$ )  $T_a = 180^{\circ}\text{C}$ , ( $+$ )  $T_a = 200^{\circ}\text{C}$ .

3. A further lower-temperature peak ( $1'$ ) which appears only at higher annealing temperatures and/or longer annealing times and strongly develops on annealing (the so-called annealing peak).

The observed features may be explained as follows: Peak 2 could correspond to more perfect but not most perfect, i.e., equilibrium, crystallites present in the original polymer as it is not affected by thermal treatments. Peak 1 could be attributed to less perfect crystals which melt at a lower temperature but would be able to perfect (e.g., during slow cooling or increasing annealing time and temperature) until their melting temperature reaches that of the stable crystals ( $T_{m2}$ ). Peak  $1'$ , introduced by

prolonged and/or higher temperature annealing and strongly dependent on the thermal history, is often interpreted as resulting from much poorer crystals grown among the larger ones. This peak may be attributed to new crystallites formed from the amorphous phase during the annealing which are less perfect and less thick than the other crystals present in the sample and increase in extent and perfection during the annealing itself, as proposed for ECTFE.<sup>13</sup>

To compare the melting behavior of ETFE to that of ECTFE, we have performed on samples of this last copolymer the following:

1. Scans at  $10^{\circ}\text{C}/\text{min}$  on samples cooled from the melt at 3, 5, 10, 20, and  $50^{\circ}\text{C}/\text{min}$  and "quenched."
2. Scans at  $10^{\circ}\text{C}/\text{min}$  on samples annealed for 1 and 2 h at 150, 180, and  $200^{\circ}\text{C}$ .

In Figure 7, reported are the DSC curves obtained on reheating at  $10^{\circ}\text{C}/\text{min}$  the samples crystallized at the different cooling rates. Two melting peaks (1 at  $T_{m1} = 230^{\circ}\text{C}$ , 2 at  $T_{m2} = 240^{\circ}\text{C}$ ) are observable up to  $v_{\text{cool}} = 10^{\circ}\text{C}/\text{min}$ , while for  $v_{\text{cool}}$  from  $20^{\circ}\text{C}/\text{min}$  to the "quenched" sample, only the higher-temperature peak at  $T_{m2} = 240^{\circ}\text{C}$  is present.

In Figure 8, the peak temperatures  $T_{m1}$  and  $T_{m2}$  are reported as a function of the cooling rate.  $T_{m1}$  increases when the cooling rate is decreased, while  $T_{m2}$  is nearly constant. The total heat of fusion  $\Delta H_m$  increases on decreasing the cooling rate (Table II).

In Figure 9 are shown the DSC curves obtained on reheating at  $10^{\circ}\text{C}/\text{min}$  the samples annealed for 1 and 2 h at 150, 180, and  $200^{\circ}\text{C}$ . At  $T_a = 150^{\circ}\text{C}$ , only peak 2 is present, while at  $T_a = 180$  and  $200^{\circ}\text{C}$

**Table I** Peak Temperatures and Heat of Fusion of ETFE Submitted to Different Thermal Treatments

Thermal History	Peak Temperatures ( $^{\circ}\text{C}$ )			Heat of Fusion (J/g) $\Delta H_m$
	$T_{m1'}$	$T_{m1}$	$T_{m2}$	
As-polymerized sample	—	—	255.4	29.06
"Quenched"	—	246.6	258.4	22.09
Crystallized from the melt at				
$10^{\circ}\text{C}/\text{min}$	—	246.4	257.0	18.47
$3^{\circ}\text{C}/\text{min}$	—	248.4	256.2	17.31
Annealed 5 h at				
$150^{\circ}\text{C}$	—	248.0	258.4	15.11
$180^{\circ}\text{C}$	203.2	—	257.8	16.12
$200^{\circ}\text{C}$	229.2	—	257.7	21.96

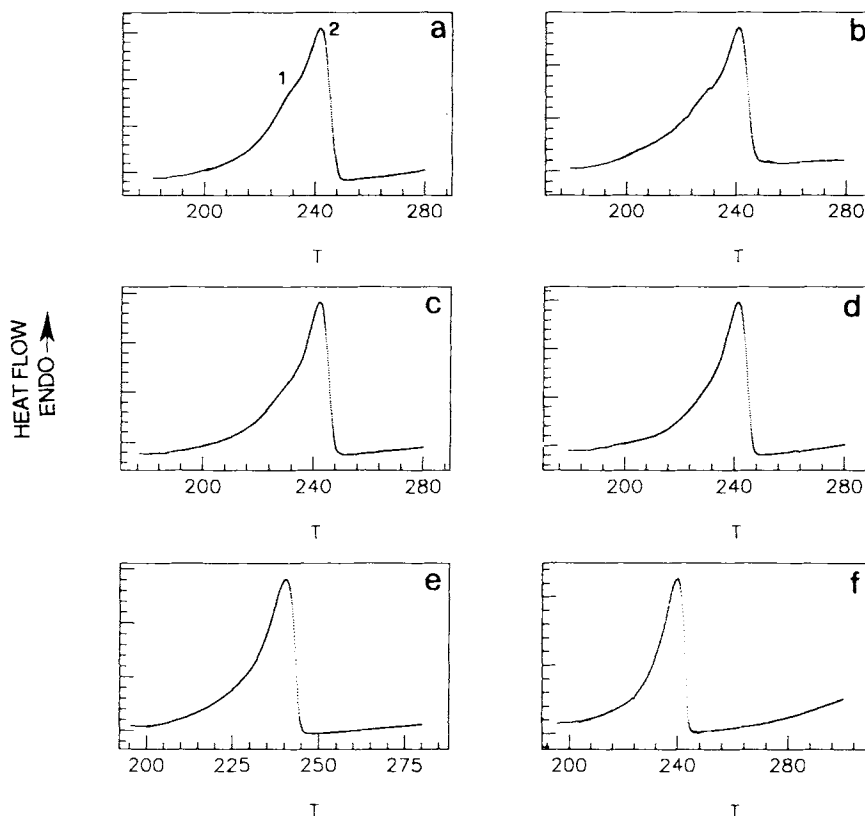


**Figure 7** DSC curves obtained on reheating at 10°C/min the samples of ECTFE crystallized from the melt at the following cooling rates: (a) 3, (b) 5, (c) 10, (d) 20, and (e) 50°C/min and (f) "quenched." Temperature is expressed in °C. Peaks 1 and 2 are shown.

from  $t_a = 1$  h, another peak 1' appears at lower temperature, whose temperature and extent increases on annealing as reported in Ref. 13.

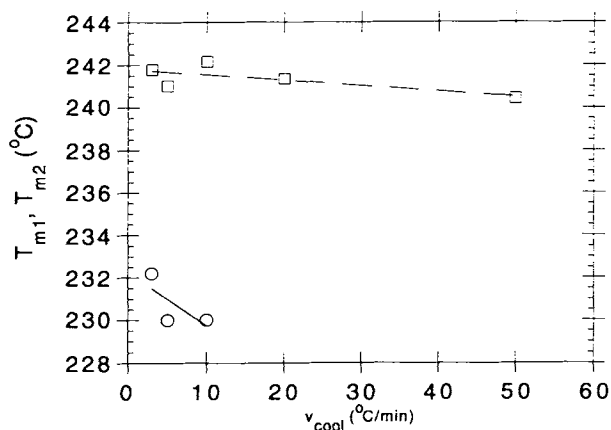


**Figure 8** Peak temperatures (°C) [(○)  $T_{m1}$ ; (□)  $T_{m2}$ ] as a function of the cooling rate (°C/min) for ECTFE.

## CONCLUSIONS

ETFE and ECTFE alternating copolymers can show three melting peaks, whose presence and extent depend upon the thermal history. The lowest-temperature peak (1') and the highest-temperature one (2) show similar features for both copolymers. Peak 2 does not depend on thermal treatments; it may be attributed to stable crystals present in the original sample. Peak 1' in both cases is produced only by annealing and strongly develops as a function of annealing time and temperature. It is the typical "annealing peak" occurring for many macromolecules several degrees above the annealing temperature and it could be due, in ETFE too, as it was proposed for ECTFE,<sup>13</sup> to new crystallites formed from the amorphous phase during annealing which perfect during the annealing itself.

Peak (1), at intermediate temperature, shows different features for the two copolymers. In fact, for ETFE, it becomes less and less important on passing from conditions of fast crystallization to slow ones

**Table II** Peak Temperatures and Heat of Fusion of ECTFE Submitted to Different Thermal Treatments

Thermal History	Peak Temperatures (°C)			Heat of Fusion (J/g) $\Delta H_m$
	$T_{m1}'$	$T_{m1}$	$T_{m2}$	
"Quenched"	—	—	239.8	24.54
Crystallized from the melt at				
10°C/min	—	230	242.2	25.90
3°C/min	—	232.2	241.8	28.23

and its temperature  $T_{m1}$  increases. Moreover, on annealing, this peak disappears and merges to that at higher temperature (2). Therefore, it could be attributed to less perfect crystals which would be fastly formed and then would be able to perfect until their melting temperature reaches that of the stable crystals. Instead for ECTFE, this peak is observed only in conditions of slow crystallization (i.e., at cooling rates equal or less than 10°C/min), while in conditions of fast crystallization, only the peak

at the highest temperature (2) is present. The decrease of  $\Delta H_m$  on increasing  $v_{cool}$  would confirm that these crystals do not form during a fast crystallization. On the basis of these considerations, also this peak, as peak 1', in ECTFE would correspond to crystallites formed from the amorphous phase. Upon annealing, this peak is no more observed because the crystals would perfect and their melting temperature would reach that of the stable crystals, as observed for ETFE.

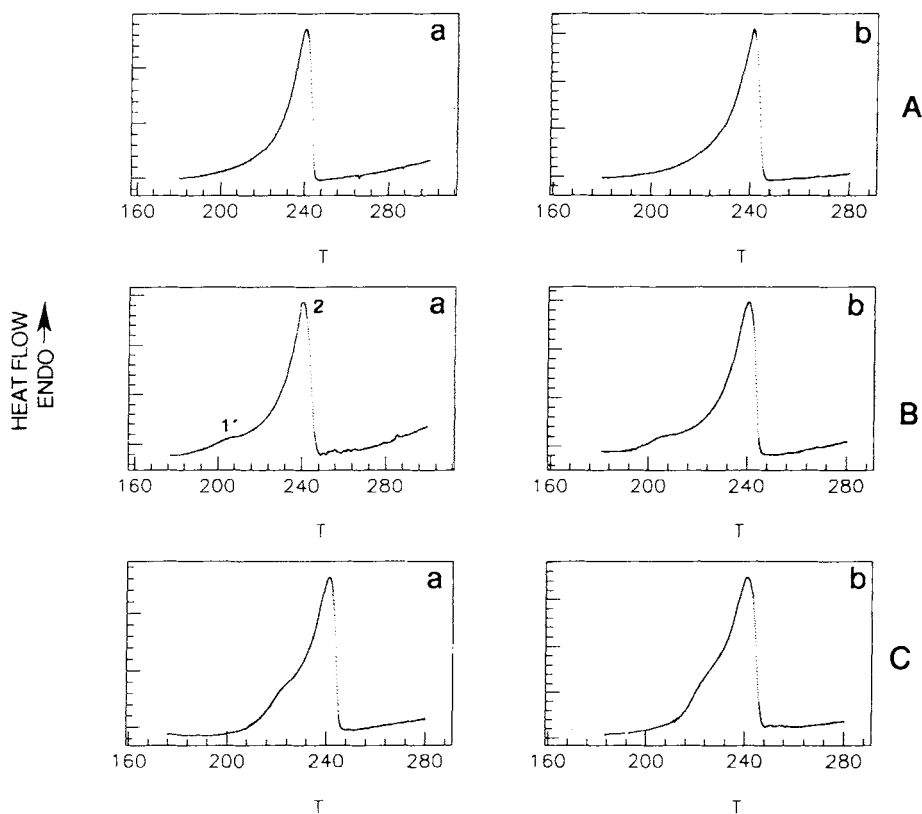


**Figure 9** DSC curves obtained on reheating at 10°C/min the samples of ECTFE annealed at (A) 150, (B) 180, and (C) 200°C for (a)  $t_a = 1$  h and (b)  $t_a = 2$  h. Temperature is expressed in °C. Peaks 1' and 2 are shown.



## REFERENCES

1. F. C. Wilson, and H. W. Starkweather Jr., *J. Polym. Sci. Polym. Phys.*, **11**, 919 (1973).
2. T. Tanigami, K. Yamaura, S. Matsuzawa, M. Ishikawa, and K. Miyasaka, *Polymer*, **27**, 999 (1986).
3. T. Tanigami, K. Yamaura, S. Matsuzawa, M. Ishikawa, and K. Miyasaka, *Polymer*, **27**, 1521 (1986).
4. K. Scheerer and W. Wilke, *Colloid Polym. Sci.*, **265**, 206 (1987).
5. G. Ajroldi and O. Pilati, Atti del II Convegno della societa' Italiana di Reologia, Siena, May 10-11, 1973.
6. M. Iuliano, C. De Rosa, G. Guerra, V. Petraccone, and P. Corradini, *Makromol. Chem.*, **190**, 827 (1989).
7. G. Guerra, C. De Rosa, M. Iuliano, V. Petraccone, P. Corradini, and G. Ajroldi, *Makromol. Chem.*, **194**, 389 (1993).
8. M. Modena, C. Garbuglio, and M. Ragazzini, *J. Polym. Sci. Polym. Lett.*, **10**, 153 (1972).
9. G. Guerra, C. De Rosa, M. Iuliano, V. Petraccone, P. Corradini, R. Pucciariello, V. Villani, and G. Ajroldi, *Makromol. Chem.*, **193**, 549 (1992).
10. J. P. Sibilial, L. G. Roldan, and S. Chandrasekaran, *J. Polym. Sci. Polym. Phys.*, **10**, 549 (1972).
11. J. P. Sibilial, R. J. Shafhauser, and L. G. Roldan, *J. Polym. Sci. Polym. Phys.*, **14**, 1021 (1976).
12. Y. P. Khanna, J. P. Sibilial, and S. Chandrasekaran, *Macromolecules*, **19**, 246 (1986).
13. Y. P. Khanna, E. A. Turi, and J. P. Sibilial, *J. Polym. Sci. Polym. Phys.*, **22**, 2175 (1984).
14. T. Suwa, T. Seguchi, M. Takehisa, and S. Machi, *J. Polym. Sci. Polym. Phys.*, **113**, 2183 (1975).
15. H. W. Starkweather, Jr., P. Zoller, J. A. Jones, and A. J. Vega, *J. Polym. Sci. Polym. Phys.*, **20**, 751 (1982).
16. S. F. Lau, H. Suzuchi, and B. Wunderlich, *J. Polym. Sci. Polym. Phys.*, **22**, 379 (1984).
17. H. W. Starkweather, *J. Polym. Sci. Polym. Phys.*, **23**, 1177 (1985).
18. E. Hellmuth, B. Wunderlich, and A. M. Rankin, *Appl. Polym. Symp.*, **2**, 101 (1966).
19. V. Villani, *Thermochim. Acta*, **162**, 189 (1990).
20. V. Villani and R. Pucciariello, *J. Therm. Anal.*, **37**, 1759 (1991).
21. V. Villani, R. Pucciariello, and G. Ajroldi, *J. Polym. Sci. Polym. Phys.*, **29**, 1255 (1991).
22. V. Villani and R. Pucciariello, *Thermochim. Acta*, **199**, 247 (1992).
23. R. Pucciariello and V. Villani, *Thermochim. Acta*, **227**, 145 (1993).
24. R. Pucciariello, *J. Polym. Sci. Polym. Phys.*, **32**, 1771 (1994).
25. B. Wunderlich, *Macromolecular Physics: Crystal Nucleation, Growth, Annealing*, Academic Press, New York, 1976, Vols. 2 and 3.

Received June 2, 1995

Accepted August 21, 1995